Low-frequency dynamics of turbulent recirculation bubbles

Laguarda, Luis; Hickel, Stefan

DOI
10.1063/5.0227332

Publication date
2024

Document Version
Final published version

Published in
Physics of Fluids

Physics of Fluids

LETTER | AUGUST 27 2024

Low-frequency dynamics of turbulent recirculation bubbles

Luis Laguarda ; Stefan Hickel

Physics of Fluids 36, 081708 (2024)
https://doi.org/10.1063/5.0227332

Physics of Fluids LETTER pubs.aip.org/aip/pof

Low-frequency dynamics of turbulent recirculation bubbles

Cite as: Phys. Fluids **36**, 081708 (2024); doi: 10.1063/5.0227332
Submitted: 8 July 2024 · Accepted: 9 August 2024 ·
Published Online: 27 August 2024

Luis Laguarda[a] and Stefan Hickel

AFFILIATIONS

Department of Flow Physics and Technology, Faculty of Aerospace Engineering, Delft University of Technology, Kluyverweg 1, Delft 2629HS, The Netherlands

[a]Author to whom correspondence should be addressed: L.LaguardaSanchez@tudelft.nl

ABSTRACT

We revisit the origin of low-frequency unsteadiness in turbulent recirculation bubbles (TRBs), and, in particular, the hypothesis of a dynamic feedback mechanism between unconstrained separation and reattachment locations. To this end, we conduct wall-resolved large-eddy simulations of a novel experimental configuration where a shock-induced TRB forms over a backward-facing step that is intended to intercept the hypothesized dynamic feedback. Our results demonstrate, for the first time, effective suppression of the low-frequency characteristics of the TRB without reducing its size, strongly supporting our hypothesis.

Oscillating loads resulting from shock-wave/turbulent boundary-layer interactions (STBLIs) pose a significant challenge in the design and operation of high-speed aerospace systems.[1] It is well-established that the shock-induced turbulent recirculation bubble (TRB) undergoes continuous expansion and contraction at very low frequencies, specifically two to three orders of magnitude lower than the characteristic frequency of integral boundary layer scales. This motion is correlated with the longitudinal excursion of the separation shock, leading to intermittent and high-amplitude thermomechanical loading on the surface. Such conditions are detrimental to the integrity of light-weight structural components, which may resonate with the unsteady loading and fail by high-cycle fatigue.

While several theories have been proposed to explain the low-frequency unsteadiness of STBLIs, associated with a separation-length based Strouhal number $St_{L_{sep}}$ smaller than ~ 0.1,[2] none of these have been conclusively supported by evidence. These theories are broadly categorized into upstream and downstream mechanisms.[3] Upstream mechanisms suggest that low-frequency dynamics arise from the passage of very large coherent structures present in the incoming turbulent boundary layer (TBL), but these structures have only been identified at high Reynolds number.[4] Downstream mechanisms, on the other hand, view the low-frequency unsteadiness as an intrinsic property of the TRB. Several models have been developed based on this idea, including an acoustic resonance mechanism in the TRB,[5] a hydrodynamic instability in the free shear layer,[6] a depleting/recharge process based on fluid entrainment by the free shear layer,[7] and the presence of centrifugal instabilities at separation and/or reattachment that continuously force the TRB.[8,9] All these mechanisms can also manifest in low-speed TRBs, which have been found to exhibit very similar low-frequency unsteadiness.[10]

While downstream mechanisms may manifest over a wide range of Reynolds and Mach numbers, it is noteworthy that only TRBs with unconstrained separation and reattachment points—meaning those with neither end fixed in the streamwise direction by the surface geometry—exhibit energetic low-frequency content. This is the case in impinging and compression-ramp STBLIs, where boundary-layer separation is induced by an adverse pressure gradient and is bound by two strong and unconstrained compressions. In contrast, forward- and backward-facing step flows do not exhibit such energetic low-frequency dynamics in the range $St_{L_{sep}} < 0.1$,[11,12] likely because either the separation or the reattachment points are geometrically constrained, i.e., fixed, in the streamwise direction by the step.

The significance of this observation should not be understated since most of the potential mechanisms hypothesized in the literature as drivers of the low-frequency unsteadiness are present in step-induced TRBs, yet their dynamic characteristics are evidently different. The new hypothesis we propose is that TRBs do not require a particular low-frequency forcing. Instead, energetic low frequencies emerge as a result of a dynamic feedback between the separation and reattachment points, which can induce hysteresis effects in the

higher-frequency oscillations of the free shear layer (occurring at $St_{Lsep} \gtrsim 0.1$[12–14]), thus leading to low-frequency unsteadiness at $St_{Lsep} < 0.1$. A necessary condition for this dynamic feedback to manifest is therefore that both the separation and reattachment points are unconstrained in the streamwise direction, which is not the case in step flows.

If our hypothesis holds, it suggests that the undesirable low-frequency content of the interaction can be suppressed by disrupting the dynamic coupling between separation and reattachment, without reducing the size of the TRB (as most control strategies aim to do) and with most of the mechanisms considered potential drivers of the low-frequency unsteadiness remaining active.

To test our hypothesis, we performed wall-resolved large-eddy simulations (LES) of a novel setup involving an impinging STBLI flow developing over a two-dimensional backward-facing step, as depicted in Fig. 1. The step is positioned at 50% of the reverse-flow region and is aimed to intercept the hypothesized dynamic coupling of the unconstrained separation and reattachment lines, potentially leading to complete decoupling at sufficiently large step heights. To assess the influence of the step height on the TRB dynamics, we investigated four different cases including the baseline interaction without a step and three step-controlled interactions with step heights of $0.35\delta_0$, $0.7\delta_0$, and $1.4\delta_0$, where δ_0 is the thickness of the undisturbed TBL at the step location.

The baseline interaction setup corresponds to the low-Reynolds interaction described in Laguarda *et al.*[15] (case $\mathcal{B}_1$). It involves an oblique shock wave (40.04°) impinging on a Mach 2.0 TBL flow with friction Reynolds number $Re_\tau = 355$ at the inviscid impingement point (labeled x_{imp}). In the step-controlled cases, the computational domain of the baseline setup is extended below the wall-plane after the step location, maintaining a constant grid spacing that corresponds to the fine wall-grid spacing of the baseline grid. All simulations are performed using the finite volume solver INCA, which employs the adaptive local deconvolution method (ALDM) for implicit LES of the compressible Navier–Stokes equations.[16] Further details on the baseline test case, numerical setup, and data collection and processing can be found in Laguarda *et al.*[15]

The influence of the step on the flow organization is first examined in Fig. 2, which shows relevant wall properties across the investigated cases. The skin-friction distributions in Fig. 2(a) show the footprint of large TRBs in all cases, with the separation point gradually moving downstream with increasing step height but still remaining upstream of the step. For the largest step, the mean separation occurs approximately $0.7\delta_0$ upstream of the step location. Furthermore, increasing the step height results in a downstream movement of the reattachment point, which increases the mean volume of the TRB by 36%, 100%, and 271%, respectively, for the different step heights. The separation lengths, determined by the first and last zero crossings of the skin-friction distribution in the streamwise direction, are $L_{sep} = 6.95\delta_0$ for the baseline case, and $6.79\delta_0$, $6.98\delta_0$, and $7.77\delta_0$ for the step-controlled interactions, in order of increasing step height. Figure 2(a) also highlights the formation of a counterclockwise recirculating bubble near each step, a feature characteristic of step flows.[11]

The mean wall-pressure distributions in Fig. 2(b) reveal a decrease in the peak pressure at reattachment as the step height increases, caused by the increasingly pronounced expansion at the step. In contrast, the mean pressure gradient at the leading edge of the interaction is less affected by the step, consistent with free-interaction theory (not shown). The peak intensity of the wall-pressure fluctuations [see Fig. 2(c)] also remains relatively consistent across all cases, despite being located closer to the step. This consistency is expected because wall-pressure fluctuations at low Reynolds number are primarily influenced by amplified vorticity fluctuations and shear layer dynamics rather than the low-frequency unsteadiness of the separation shock.[15] Downstream of the interaction, the observed increase in wall-pressure fluctuation intensity is attributed to reattaching shear layer vortices, and it exhibits similar levels across all cases.

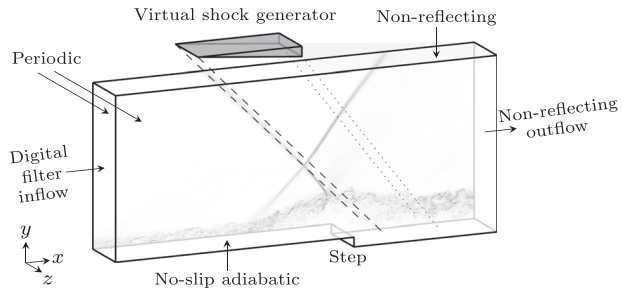

FIG. 1. Schematics of the computational domain.

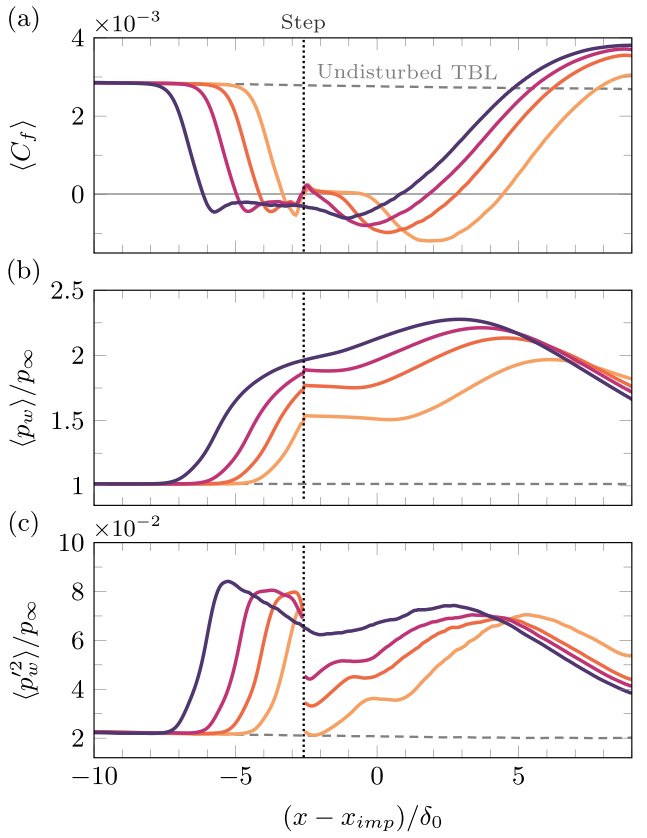

FIG. 2. Time- and spanwise-averaged (a) skin-friction, (b) wall pressure, and (c) wall-pressure fluctuation intensity. Color legend: (purple curve) baseline interaction (no-step case); (other colors) step-controlled interactions with a step height of (magenta curve) $0.35\delta_0$, (red curve) $0.7\delta_0$, and (orange curve) $1.4\delta_0$.

Differences in flow organization are further highlighted in Fig. 3, which depicts contours of pressure fluctuations and streamwise-velocity fluctuations for both the baseline interaction and the step-controlled interaction with the intermediate step. Notably, the presence of the step results in attenuated pressure fluctuations at the separation shock and the detaching shear layer. A similar effect is observed for the streamwise-velocity fluctuations, except at the separation-shock foot, where the peak intensity is predominantly influenced by the mean flow deceleration induced by the pressure gradient,[15] and thus remains relatively unaffected by the step. The separation-shock angle also remains approximately constant across all cases, consistent once again with predictions from free-interaction theory.

The isocontours of zero streamwise velocity (magenta line) reveal a clear difference in the shape of the bubble. In the larger step-controlled cases, the reverse-flow region remains shallow and confined close to the wall before the step. This suggests that the step effectively divides the separation region into two distinct compartments, with significant mixing with the outer flow and fluid entrainment occurring only downstream of the step, where the reverse flow is not confined to the wall. Such a condition potentially facilitates the decoupling of separation and reattachment, which is the primary objective of the present experiments.

To substantiate this observation, we evaluate the crucial aspect of unsteadiness in the investigated TRBs through spectral analysis of wall-pressure signals for each case, depicted in Figures 4(a)–4(d) as pre-multiplied power spectral density (PSD) plots. These plots unequivocally demonstrate that the prominent low-frequency component present around the separation-shock foot in the baseline interaction (at $St_{L_{sep}} < 0.1$) diminishes progressively with increasing step height. This reduction is evident not only near the separation point but also within the recirculation region and near the reattachment point. Consequently, the observed changes in the shape of the TRB correlate strongly with the suppression of low-frequency dynamics, thus supporting our hypothesis.

To confirm the effective suppression of low-frequency dynamics beyond their mere attenuation at the wall, we also examined the pre-multiplied PSD of the spanwise-averaged separation-shock location for each case, tracked above the TBL. These results are shown in Fig. 4(e), where the step height increases from top to bottom. Consistent with the wall-pressure PSDs and the two-dimensional contours in Fig. 3, these spectra clearly illustrate a progressive decrease in the separation-shock motion at low frequencies ($St_{L_{sep}} < 0.1$) with increasing step height. Since the incoming boundary layer turbulence is identical for all cases, we can rule out upstream mechanisms as the cause of low-frequency unsteadiness.

We have also analyzed the two-dimensional zero time lag cross correlation of wall-pressure fluctuations with the reattachment location as a reference point. The results, shown in Fig. 5(a) with step height increasing from top to bottom, confirm that wall-pressure fluctuations at the separation and reattachment locations are no longer anti-correlated in the larger step cases. This is evident from the absence of a significant correlation around the mean separation location, which is indicated by a dashed line.

Additionally, Fig. 5(b) presents cross correlation maps computed with skin-friction fluctuations, and these confirm the presence of streaky structures beyond reattachment in all cases. Previous works identify these streaks as the imprint of streamwise-aligned vortices—often referred to as Görtler-like vortices—at reattachment.[8,9] Although their exact role in the low-frequency dynamics of the TRB remains inconclusive, our results show that these structures persist even when low-frequency dynamics are suppressed. This suggests that streamwise-aligned vortices either do not play a pivotal role in such dynamics, or they must originate from strong concave streamline curvature at separation to be dynamically significant, a condition that is absent in the large-step-controlled TRBs.

To summarize, we have provided evidence that the low-frequency dynamics of TRBs may originate from a dynamic coupling between unconstrained separation and reattachment lines. This coupling can be

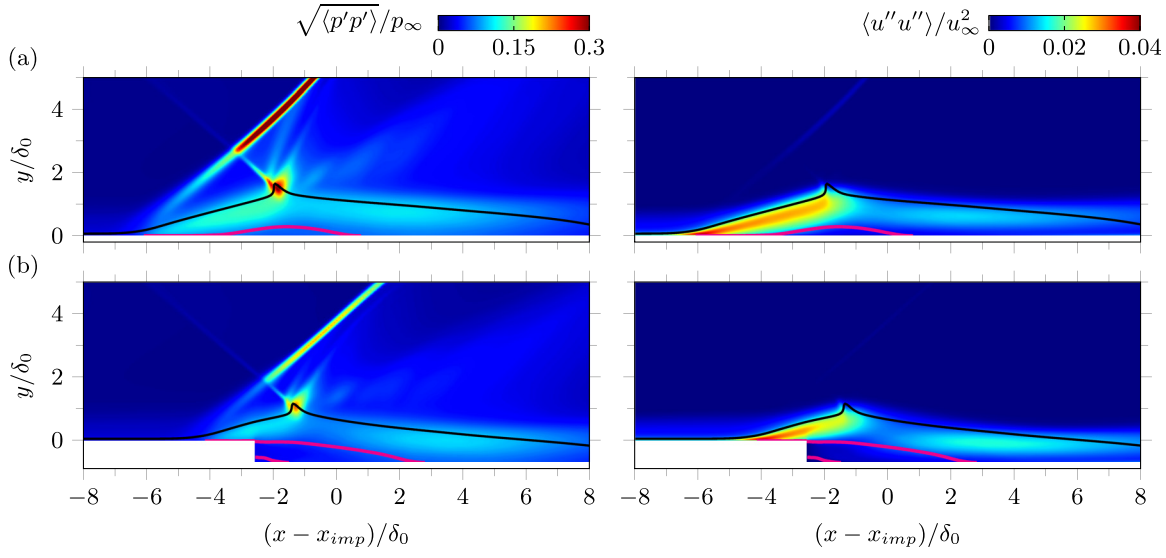

FIG. 3. Pressure fluctuation intensity (left) and streamwise velocity fluctuations (right) for (a) the baseline interaction (no-step case) and (b) the step-controlled interaction with a step height of $0.7\delta_0$. Magenta and black lines, respectively, indicate the time- and spanwise-averaged separation line ($\langle u \rangle = 0$) and sonic line ($\langle M \rangle = 1$).

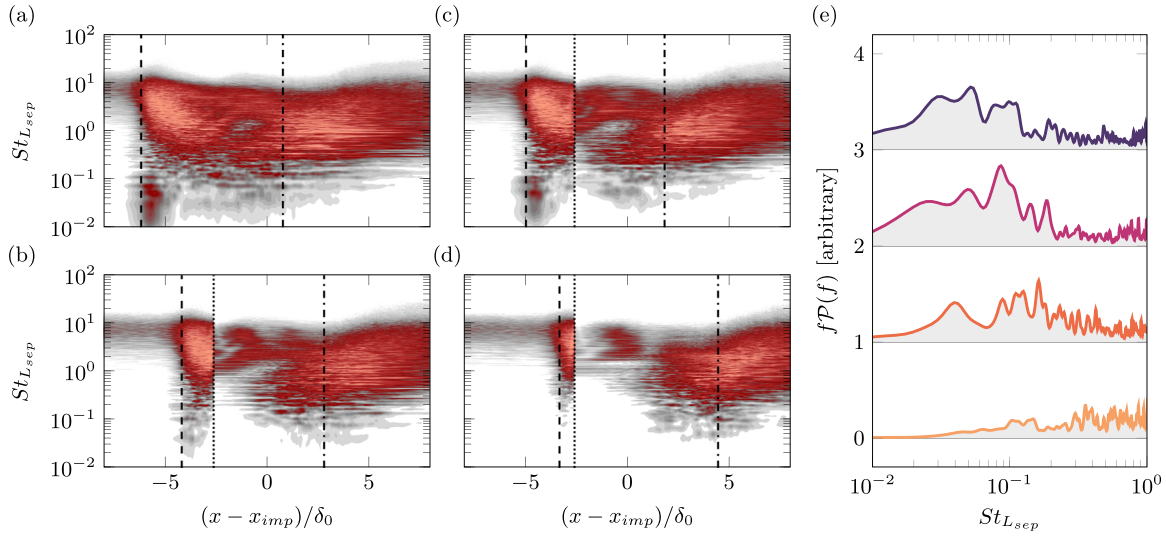

FIG. 4. Pre-multiplied PSD of (a)–(d) wall-pressure fluctuations and (e) spanwise-averaged separation-shock location tracked above the TBL. The step height increases from (a) to (d), and its location is indicated by a dotted line. The mean separation and reattachment locations in these panels are marked by dashed and dashed-dotted lines, respectively, and the color map ranges linearly from light gray to light red. In (e), the step height increases from top to bottom, with spectra offset for clarity (refer to the caption of Fig. 2 for the line legend).

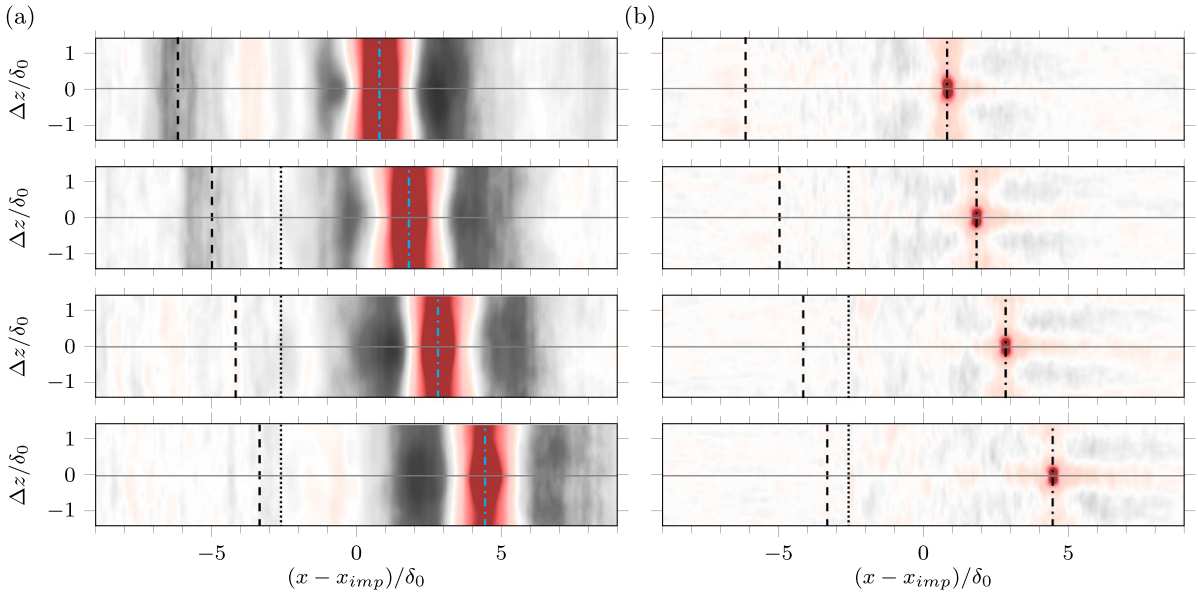

FIG. 5. Two-dimensional zero time lag cross correlation $R(x, \Delta z)$ referenced to the reattachment location (dashed-dotted line) for (a) wall-pressure fluctuations and (b) skin-friction fluctuations. The step height increases from top to bottom, and the colormap ranges from $R = -0.3$ (gray) to $R = 0.3$ (red). Refer to the caption of Fig. 4 for additional details.

effectively intercepted by placing a backward-facing step underneath the TRB, a strategy not previously explored in the literature. The pronounced expansion at the step is found to progressively alter the flow topology of the TRB as the step height increases, keeping the reverse-flow region shallow and confined close to the wall upstream of the step. This alteration allows mixing and fluid entrainment to be significant only downstream of the step, effectively compartmentalizing the TRB. We show that this compartmentalization strongly correlates with the overall suppression of low-frequency dynamics, thereby supporting our hypothesis about their origin.

AUTHOR DECLARATIONS

Conflict of Interest

The authors have no conflicts to disclose.

Author Contributions

Luis Laguarda: Conceptualization (equal); Formal analysis (equal); Investigation (equal); Software (equal); Writing – original draft (equal); Writing – review & editing (equal). **Stefan Hickel:** Conceptualization (equal); Investigation (equal); Software (equal); Writing – review & editing (equal).

DATA AVAILABILITY

The data that support the findings of this study are available upon request.

REFERENCES

[1]J. M. Delery, "Shock wave/turbulent boundary layer interaction and its control," Prog. Aerosp. Sci. **22**, 209–280 (1985).
[2]J.-P. Dussauge, P. Dupont, and J.-F. Debiève, "Unsteadiness in shock wave boundary layer interactions with separation," Aerosp. Sci. Technol. **10**, 85–91 (2006).
[3]N. T. Clemens and V. Narayanaswamy, "Low-frequency unsteadiness of shock wave/turbulent boundary layer interactions," Annu. Rev. Fluid Mech. **46**, 469–492 (2014).
[4]B. Ganapathisubramani, N. T. Clemens, and D. S. Dolling, "Large-scale motions in a supersonic turbulent boundary layer," J. Fluid Mech. **556**, 271–282 (2006).
[5]S. Pirozzoli and F. Grasso, "Direct numerical simulation of impinging shock wave/turbulent boundary layer interaction at M = 2.25," Phys. Fluids **18**, 065113 (2006).
[6]M. Wu and M. P. Martin, "Analysis of shock motion in shockwave and turbulent boundary layer interaction using direct numerical simulation data," J. Fluid Mech. **594**, 71–83 (2008).
[7]S. Piponniau, J.-P. Dussauge, J.-F. Debieve, and P. Dupont, "A simple model for low-frequency unsteadiness in shock-induced separation," J. Fluid Mech. **629**, 87–108 (2009).
[8]S. Priebe, J. H. Tu, C. W. Rowley, and M. P. Martín, "Low-frequency dynamics in a shock-induced separated flow," J. Fluid Mech. **807**, 441–477 (2016).
[9]V. Pasquariello, S. Hickel, and N. A. Adams, "Unsteady effects of strong shock-wave/boundary-layer interaction at high Reynolds number," J. Fluid Mech. **823**, 617–657 (2017).
[10]A. Mohammed-Taifour and J. Weiss, "Unsteadiness in a large turbulent separation bubble," J. Fluid Mech. **799**, 383–412 (2016).
[11]W. Hu, S. Hickel, and B. W. Van Oudheusden, "Low-frequency unsteadiness mechanisms in shock wave/turbulent boundary layer interactions over a backward-facing step," J. Fluid Mech. **915**, A107 (2021).
[12]F. F. J. Schrijer, A. Sciacchitano, and F. Scarano, "Spatio-temporal and modal analysis of unsteady fluctuations in a high-subsonic base flow," Phys. Fluids **26**, 086101 (2014).
[13]M. C. Adler and D. V. Gaitonde, "Dynamic linear response of a shock/turbulent-boundary-layer interaction using constrained perturbations," J. Fluid Mech. **840**, 291–341 (2018).
[14]L. M. Hudy, A. M. Naguib, and W. M. Humphreys, Jr., "Wall-pressure-array measurements beneath a separating/reattaching flow region," Phys. Fluids **15**, 706–717 (2003).
[15]L. Laguarda, S. Hickel, F. F. J. Schrijer, and B. W. Van Oudheusden, "Reynolds number effects in shock-wave/turbulent boundary-layer interactions," J. Fluid Mech. **989**, A20 (2024).
[16]S. Hickel, C. P. Egerer, and J. Larsson, "Subgrid-scale modeling for implicit large eddy simulation of compressible flows and shock-turbulence interaction," Phys. Fluids **26**, 106101 (2014).